

Electronic supplementary information

Effect of Mg substitution on $\text{LaTi}_{1-x}\text{Mg}_x\text{O}_{3+\delta}$ catalysts for improving C2
selectivity of the oxidative coupling of methane

Larissa de Bessa Lopes^a, Luiz H. Vieira^a, José Mansur Assaf^b, Elisabete Moreira

Assaf^{*a}

^a University of São Paulo, São Carlos Institute of Chemistry, Av. Trabalhador São-carlense, 400,
13560-970 São Carlos, Brazil.

^b Federal University of São Carlos, Rod. W. Luiz, km.235, São Carlos, SP, Brazil.

*E-mail: eassaf@iqsc.usp.br

1. Supplementary information on experimental

Synthesis of pure oxide catalysts

Pure oxide catalysts (La_2O_3 , TiO_2 e MgO) were prepared by the polymerized complex method. 0.2 moles of each cation precursor (lanthanum nitrate, titanium isopropoxide or magnesium nitrate) were added to 4 moles of ethylene glycol and 1 mol of anhydrous citric acid under constant stirring. The solution was stirred for 30 min at ambient temperature and then heated at 120 °C until full polymerization. The polymer was calcined at 300 °C for 2 h, macerated and calcined at 800 °C for 4 h.

XPS analyses

The inelastic background of the La 3d, Ti 2p, Mg 2s, C 1s, and O 1s spectra was subtracted using Shirley's equation. The binding energy scale of the spectra was corrected using the C1s hydrocarbon group (284.8 eV). The atomic composition of the surface layer (<5 nm) was determined by the relative proportions of the areas of the spectra corrected by Scofield's atomic sensitivity factors, with an accuracy of $\pm 5\%$. The spectra were deconvolved using a Voigtian function, with Gaussian (70%) and Lorentzian (30%) combinations.

CO₂-TPD analyses

The catalysts samples (200 mg) were heated in Ar flow (50 mL.min⁻¹ and 10 °C.min⁻¹ heating rate) from 30 to 800 °C and then cooled to 30 °C. After this step, the samples were treated with CO₂ flow (30 mL.min⁻¹) for 1 h and Ar flow (20 mL.min⁻¹) for 30 min. Finally, the Ar flow was maintained for recording the CO₂-TPD results, and the samples were heated at 5°C.min⁻¹ from 30°C to 800°C and held at this temperature until the curve returned to the baseline.

DRIFTS analyses

The catalysts were heated in He flow (20 mL.min⁻¹) up to 500 °C and held for 30 min; they were then cooled to 50 °C and kept under CO₂ flow (20 mL.min⁻¹) for 30 min, followed by He flow (20 mL.min⁻¹) for 15 min. The spectra were collected after this step, and the processes were repeated for the chemisorption at 300 and 500 °C. The background spectra at each temperature were obtained before the CO₂-chemisorption. Data were treated by the Smooth and Kubelka Munk functions.

2. Supplementary information on results

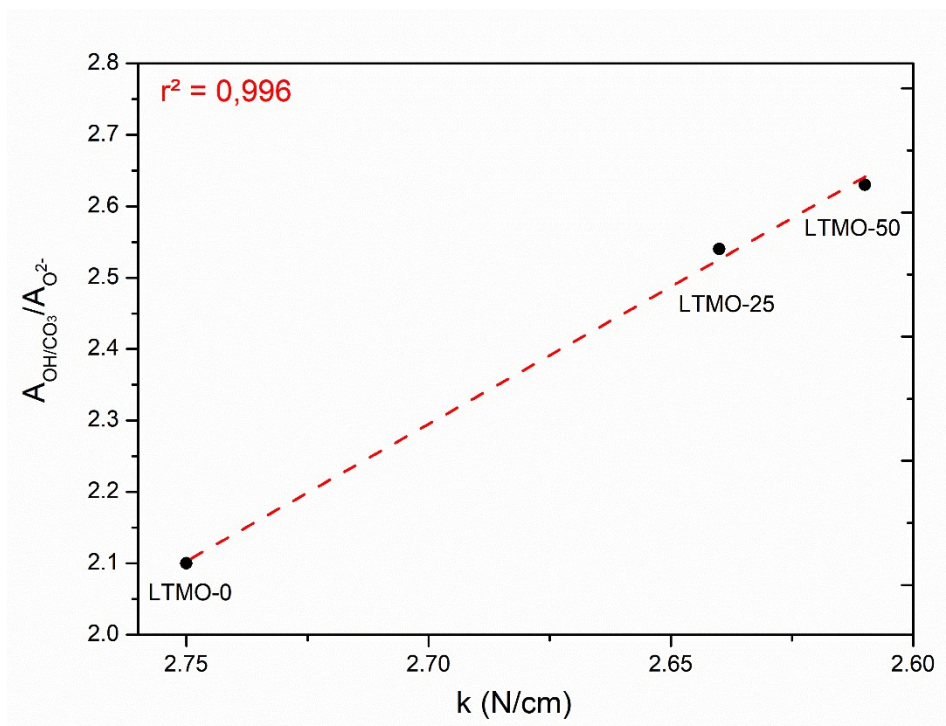


Figure S1. The ratio of hydroxyl/carbonate oxygen and lattice oxygen ($A_{\text{OH}/\text{CO}_3}/A_{\text{O}_2^-}$) versus bond force constant. A linear fit was performed with $r^2 = 0.996$.

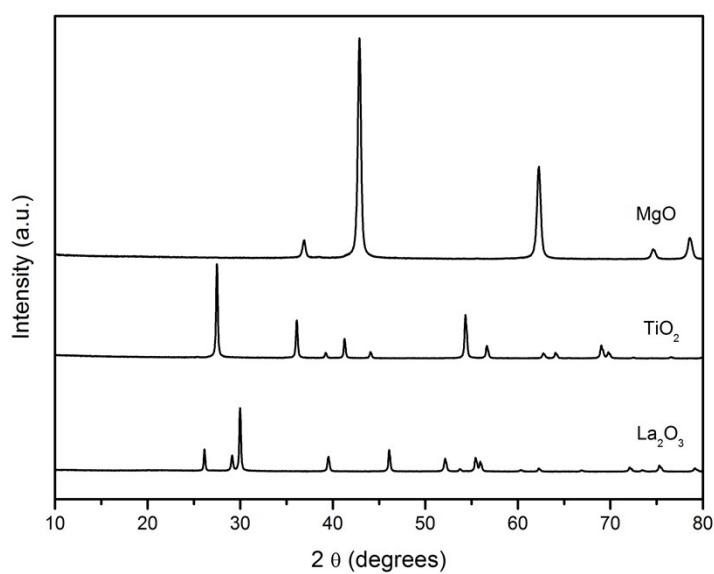


Figure S2. X-ray diffraction patterns of La_2O_3 , TiO_2 and MgO catalysts.

The patterns for all pure oxide structures were verified by X-ray diffraction analysis (Fig. S1). Lanthanum oxide (PDF No. 05-0602) showed diffraction patterns corresponding to a hexagonal crystalline system and $P-3m1$ space group. Titanium oxide (PDF No. 71-0650) was formed in a rutile crystalline structure (tetragonal, $P42 / mnm$), and magnesium oxide (PDF No. 45-0946) was formed in a periclase crystalline structure (cubic, $Fm -3m$).

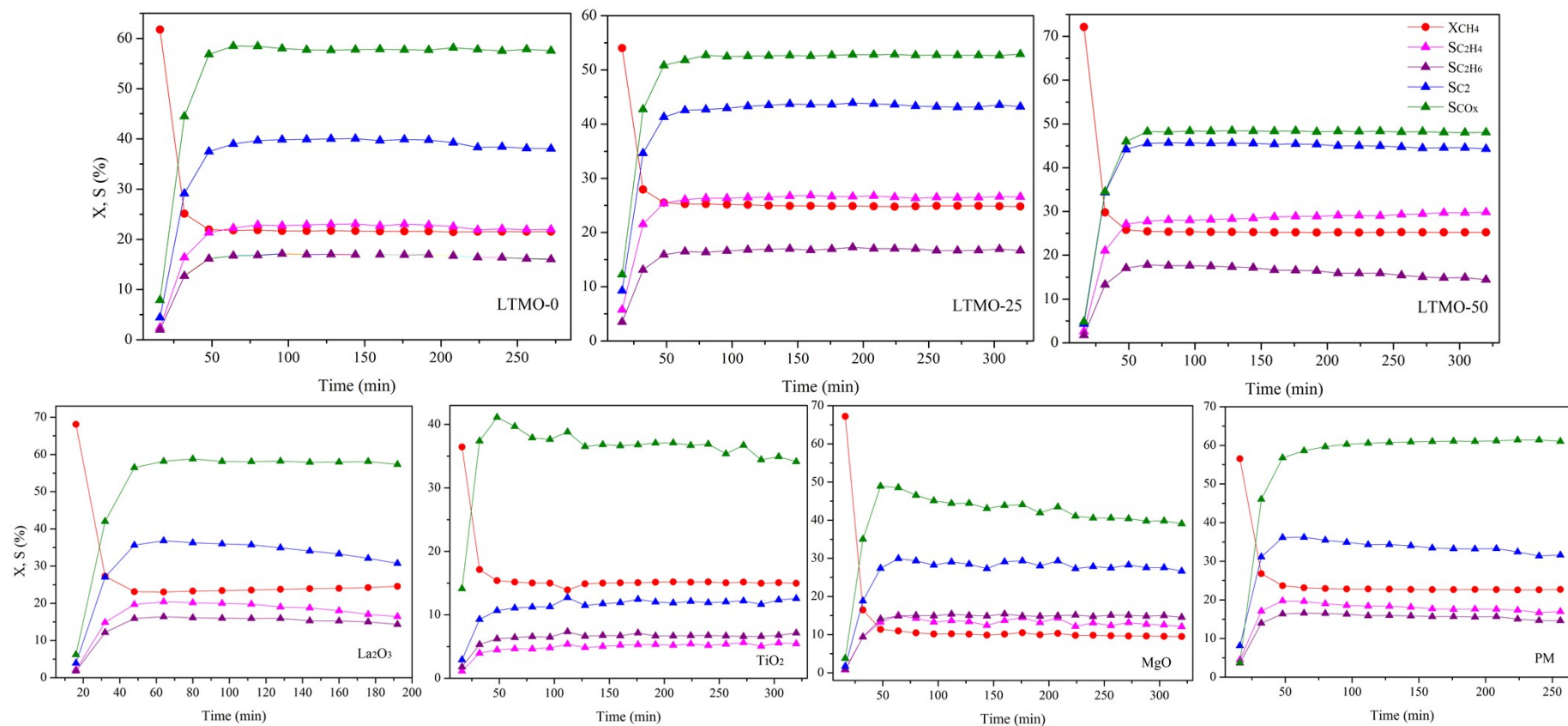


Figure S3. Methane conversion (X_{CH_4}), CO_x selectivity (S_{CO_x}), C_2H_4 selectivity ($S_{C_2H_4}$), C_2H_6 selectivity ($S_{C_2H_6}$) and C_2 selectivity (S_{C_2}) over the OCM reaction time for LTMO-0, LTMO-25, LTMO-50, La_2O_3 , TiO_2 , MgO and PM. Reaction conditions: $CH_4/O_2 = 8$, $W = 45000 \text{ mL}_{cat}^{-1} \cdot h^{-1}$ and $T = 800 \text{ }^\circ\text{C}$.

Table S1. Catalytic performance of LTMO-50 catalyst and other perovskite structures of OCM literature.

Catalysts	X_{CH_4} (%)	S_{C_2} (%)	$\text{C}_2\text{H}_4/\text{C}_2\text{H}_6$	GHSV (h^{-1})	T ($^\circ\text{C}$)	CH_4/O_2	S_{BET} (m^2/g)	Productivity	
								$\text{mmol}_{\text{C}_2}\cdot\text{g}^{-1}\cdot\text{h}^{-1}$	$\text{mmol}_{\text{C}_2}\cdot\text{m}^{-2}\cdot\text{h}^{-1}$
LTMO-50	17.3	51.4	0.97	30,000 ^a	800	8	5.0	68.2	13.6
$\text{La}_2\text{Ti}_2\text{O}_7$ ¹	18	32	0.5	18,000 ^a	800	4	16.3	18.9	1.2
LaAlO_3 ²	24	44	0.6	10,000	800	4	3.0	4.4 ^b	1.5
LaFeO_3 ²	18	19	1.4	10,000	800	4	3.0	1.5 ^b	0.5
LaNiO_3 ²	14	2	3	10,000	700	4	3.3	0.1 ^b	0.03
BaSrTiO_3 ³	47	29.5	-	6,000	800	2	4.4	17.0	3.9
MgBaSrTiO_3 ³	46.5	43	-	6,000	800	2	0.9	29.5	32.7
SrTiO_3 ⁴	15	62.6	2	151,200	850	4	1.5	115.3 ^b	76.8
$\text{SrTi}_{0.9}\text{Mg}_{0.1}\text{O}_3$ ⁴	24	64	1.3	151,200	850	4	3.2	188.6 ^b	58.9

a. WHSV ($\text{mL}\cdot\text{g}^{-1}\cdot\text{h}^{-1}$)

b. catalyst mass was calculated from catalyst volume using the following densities: $\text{LaAlO}_3 = 6.52 \text{ g/cm}^3$; $\text{LaFeO}_3 = 6.40 \text{ g/cm}^3$; $\text{LaNiO}_3 = 6.93 \text{ g/cm}^3$; $\text{SrTiO}_3 = 4.81 \text{ g/cm}^3$.

3. References for supplementary material

- 1 J. Xu, Y. Zhang, X. Xu, X. Fang, R. Xi, Y. Liu, R. Zheng and X. Wang, *ACS Catal.*, 2019, **7**, 4030–4045.
- 2 I. Kim, G. Lee, H. Bin Na, J. M. Ha and J. C. Jung, *Mol. Catal.*, 2017, **435**, 13–23.
- 3 Z. Fakhroueian, F. Farzaneh and N. Afrookhteh, *Fuel*, 2008, **87**, 2512–2516.
- 4 D. V. Ivanov, L. A. Isupova, E. Y. Gerasimov, L. S. Dovlitova, T. S. Glazneva and I. P. Prosvirin, *Appl. Catal. A Gen.*, 2014, **485**, 10–19.